ATATÜRK ÜNİVERSİTESİ YAYINLARI
ATATURK UNIVERSITY PUBLICATIONS

Research Article *Araştırma Makalesi* DOI: 10.5281/zenodo.16415659

Numerical Optimization of Operating Parameters in a Photovoltaic Drying System

Fotovoltaik Destekli Kurutma Sisteminde İşletme Parametrelerinin Sayısal Optimizasyonu

Rıdvan YAKUT
Kafkas University, Faculty of Engineering, Architecture, Department of Mechanical Engineering, Kars, Türkiye

Rahim Aytuğ ÖZER
Erzurum Technical University, Faculty of Engineering, Architecture, Department of Aerospace Engineering, Erzurum, Türkiye

Jülide ERKMEN
Kafkas University, Faculty of Engineering, Architecture, Department of Chemical Engineering, Kars, Türkiye

ABSTRACT

In this study, the effects of the evaporator design on the thermal and fluid performance of photovoltaic-assisted solar drying systems were investigated using numerical methods. To optimize the temperature and mass flow rate of the air supplied to the drying system, Computational Fluid Dynamics (CFD) analyses were performed on evaporator models with different channel heights (3, 4, and 5 cm) under three different mass flow rate conditions (0.025, 0.050, and 0.075 kgs^{-1}). The obtained temperature contours and streamline patterns revealed that, particularly at a channel height of 3 cm and mass flow rate of 0.075 kgs^{-1}, the airflow made more effective contact with the surface, maximizing heat transfer. In contrast, for the 4 cm and 5 cm channels, the airflow moved away from the surface, leading to a reduced cooling performance and increased production costs. Considering the average outlet temperature and velocity values, the best performance was achieved with a 3 cm channel height and 0.075 kgs^{-1} mass flow rate configuration. Therefore, to enhance the efficiency of solar-powered drying systems, it is recommended to design an evaporator with a 3 cm channel height and operate it under high flow conditions. This study provides a valuable technical reference for engineers and researchers for the design of PV-based drying systems.

Keywords: Evaporator, drying system efficiency, thermal-fluid analysis, CFD

ÖZ

Bu çalışmada, fotovoltaik (PV) destekli güneş enerjili kurutma sistemlerinde evaporatör tasarımının ısıl ve akışkan performansı üzerindeki etkileri sayısal yöntemlerle incelenmiştir. Kurutma sistemine verilen havanın sıcaklık ve kütlesel debisinin optimize edilmesi amacıyla, farklı kanal yüksekliklerine (3, 4 ve 5 cm) sahip evaporatör modelleri için üç farklı kütlesel debi (0.025, 0.050 ve 0.075 kgs^{-1}) koşulunda Hesaplamalı Akışkanlar Dinamiği (HAD) analizleri gerçekleştirilmiştir. Elde edilen sıcaklık konturları ve akış çizgileri, özellikle 3 cm kanal yüksekliği ve 0.075 kgs^{-1} debi kombinasyonunda hava akışının yüzeyle daha etkin temas sağladığını ve bunun da ısı transferini maksimize ettiğini göstermiştir. Buna karşın, 4 cm ve 5 cm'lik kanallarda hava akımı yüzeyden uzaklaştığı için soğutma performansında azalma ve üretim maliyetlerinde artış gözlemlenmiştir. Ortalama çıkış sıcaklığı ve hız değerleri dikkate alındığında, en iyi performans 3 cm kanal yüksekliği ve 0.075 kgs^{-1} hava debisiyle elde edilmiştir. Bu nedenle, güneş enerjisiyle çalışan kurutma sistemlerinin verimliliğini artırmak amacıyla 3 cm kanal yüksekliğine sahip bir evaporatör tasarımı önerilmekte ve sistemin yüksek hava debisiyle çalıştırılması tavsiye edilmektedir. Bu çalışma, PV tabanlı kurutma sistemlerinin tasarımı konusunda mühendis ve araştırmacılar için teknik bir referans niteliği taşımaktadır.

Anahtar Kelimeler: Evaporatör, kurutma sistemi verimliliği, ısıl-akışkan analizi, HAD

Received/Geliş Tarihi : 26.05.2025
Revision/Revizyon Tarihi: 25.06.2025
Accepted/Kabul Tarihi : 25.06.2025
Publication Date/Yayın Tarihi : 31.07.2025

Corresponding Author/Sorumlu Yazar:
E-mail: ryakut@kafkas.edu.tr

Cite this article: Yakut R., Özer, R. A., & Erkmen, J. (2025). Numerical Optimization of Operating Parameters in a Photovoltaic Drying System. *Journal of Energy Trends*, 2(1) 13-20

Introduction

Drying is considered a fundamental technology in the agricultural and food industries for product preservation, facilitating logistics, and adding value. It is a suitable method for preserving fruits and vegetables due to their limited shelf life, and dried products are used as ingredients in the pharmaceutical, cosmetic, and snack sectors (Arpaci et al., 2024). In developing countries, there is a growing interest in drying systems based on renewable energy sources to reduce energy costs and promote environmental sustainability (Belessiotis & Delyannis, 2011; Ahmad Fudholi et al., 2014). In this context, solar drying systems stand out because of their low operating costs, environmental friendliness, and technical simplicity (Shalaby et al., 2014a).

Solar dryers can be designed as direct, indirect, or hybrid drying systems, depending on the application type (Kerse et al., 2025; Shalaby et al., 2014a). Although traditional open-air drying methods offer advantages, such as low initial investment and no energy requirement, they have significant limitations in terms of product quality and hygiene. The inability to control environmental parameters such as temperature, humidity, and radiation in these systems prolongs the drying process and increases microbiological risks (El-Sebaii & Shalaby, 2012; Esper & Mühlbauer, 1998). Furthermore, external factors such as dust, insects, mold spores, and animal contact elevate the risk of product contamination, thereby posing a serious threat to food safety (Ertekin & Yaldiz, 2004; Sodha & Chandra, 1994). Due to uneven drying, over-drying in some parts and moisture retention in others often leads to deterioration in sensory qualities such as color, aroma, and texture (Ertekin & Yaldiz, 2004; Sodha & Chandra, 1994). Enclosed solar drying systems that provide a controlled and hygienic environment have emerged as a more sustainable, reliable, and quality-focused alternative to traditional methods. These systems remove moisture through natural or fan-assisted airflow, thereby preserving product quality. In modern solar dryers, structural enhancements such as multi-pass air channels, thermal mass integration, and mesh or finned absorber modifications have been implemented to improve energy efficiency (Abdullah et al., 2018; Fadhel et al., 2010; Güler et al., 2020). Moreover, the use of numerical analysis methods, such as computational fluid dynamics (CFD), allows for the optimization of thermal performance and enhances design accuracy (Keshani et al., 2015; Sanghi et al., 2018). CFD is a valuable alternative for estimating convective transfer coefficients and is used in drying studies in the literature (Souza et al., 2023; Tu et al., 2023). These systems also offer an effective drying solution when direct exposure of the product to sunlight is not desired or feasible (Mustayen et al., 2014).

Various studies have demonstrated the effective use of solar energy systems for drying food products. In a study conducted by Barnwal & Tiwari (2008), a greenhouse-type photovoltaic drying system was designed to dry seedless grapes. The amount of evaporated moisture was determined, and heat and mass transfer analyses were performed. Based on the results obtained for different greenhouse configurations, the convective heat transfer coefficient was reported to range between 0.26 and 0.97 $Wm^{-1}K^{-1}$. In another study conducted by Ghafar et al. (2025), a photovoltaic drying system was developed for mullet. In this system, hot air is applied using both natural and forced convection, and its performance is evaluated. The results showed that the forced convection system achieved an efficiency of 85.78%, whereas natural air circulation provided an efficiency of 59.36%. In terms of the moisture removal capacity, forced convection was 36%, whereas natural convection was 22%. The authors also emphasized that the drying rate was significantly higher in the forced convection system than in the natural convection system.

The main barrier to the widespread use of solar-powered drying systems in the agricultural sector is their high initial installation costs. However, studies in this field have shown that compared to traditional open-field drying methods, solar dryers can be more economical in the long term. Solar dryers offer financial advantages for high-value agricultural products, and high-cost systems can be justified under such conditions (Bal et al., 2011). Today, it is possible to manufacture low-cost solar drying systems using locally available and inexpensive materials (Bal et al., 2011). Sharma et al. (2009) conducted studies on simple and low-cost dryers that can be easily used in rural areas or small-scale production units. A. Fudholi et al. (2010) also provided examples regarding the local manufacturing possibilities and costs of such systems.

Another major limitation of solar drying technology is its reliance on sunny periods for operation. This constraint reduces the efficiency of the system and limits its usable time. To overcome this issue, next-generation solar dryers supported by thermal energy storage systems are being developed. These systems enable the continued drying process, even in the absence of sunlight, thereby ensuring operational continuity. In this context, Bal et al. (2011) demonstrated the positive impact of energy storage technologies on continuous system operation in their research. Furthermore, Shalaby et al. (2014b) conducted a detailed investigation of systems utilizing phase change materials (PCMs). They emphasized that latent heat storage methods, particularly those involving PCMs, help reduce energy losses and significantly enhance the overall system efficiency.

One of the most notable aspects of solar drying systems is that they operate entirely on renewable energy sources and offer an environmentally friendly drying method. Additionally, because these systems can be constructed using locally available materials, they hold significant value in terms of rural development and sustainability. Current research clearly demonstrates that solar drying technology has the potential to reduce environmental impact and support sustainable agriculture.

In this study, the operating parameters that influence the thermal and fluid dynamic performances of photovoltaic-assisted solar drying systems were identified, and the system design was optimized accordingly. For this purpose, the drying unit was modeled in three dimensions using CFD with ANSYS Fluent software. During the modeling process, the effects of critical design parameters, particularly the evaporator height and the air mass flow rate supplied to the system, on the drying efficiency were examined in detail. Despite significant advances in drying research, further studies are needed to optimize drying conditions based on CFD-integrated models for multiple samples, focusing on achieving uniform air velocity as well as moisture and temperature distributions across samples (Hassan et al., 2025). In this context, the present study contributes to the existing literature by providing a detailed CFD-based analysis of drying performance under various operating conditions.

As a result of the optimization study, the most suitable configurations were determined under different operating conditions in terms of energy efficiency and drying duration. These findings serve as both a theoretical and practical guide for researchers aiming to design more effective and sustainable PV-based drying systems. In this respect, this study significantly contributes to the advancement of drying technologies that seek to maximize the benefits of solar energy.

Materials and Methods

In this study, numerical analyses were conducted on evaporators with three channel heights (3, 4, and 5 cm). For each geometric configuration, three mass flow rates (0.025, 0.050, and 0.075 kgs^{-1}) were considered, resulting in nine different scenarios. In all the simulations, a constant heat flux boundary condition was applied to the evaporator surface to evaluate the heat transfer performance. Numerical modeling was performed using the commercial CFD software ANSYS Fluent.

Given the nature of the flow regime, it was assumed to be turbulent, and the standard k–ε turbulence model was selected because of its proven ability to accurately represent the wall jet behavior. This model has been shown in previous studies to yield reliable results for flows with high Reynolds numbers (Yakut et al., 2016).

Because the evaporator geometry was symmetric, the computational domain was reduced by half using symmetric modeling, which significantly lowered the computational cost while allowing for a denser and more accurate mesh structure. To enhance the accuracy of the numerical solution, a hybrid meshing approach was employed by combining structured and unstructured meshes to effectively resolve the geometrically complex regions. Tetrahedral elements are preferred in these regions owing to their superior adaptability. The mesh quality was optimized by maintaining an aspect ratio close to one and minimizing the skewness values (Ozer, 2025).

During the solution process, the conservation equations for mass, momentum, and energy were solved with appropriate boundary conditions. The following assumptions were made in the simulations.

1. The thermophysical properties of the fluid (air) were assumed to be constant.
2. The flow was steady state, incompressible, and three-dimensional.
3. The buoyancy and radiative heat transfer effects were neglected.
4. The heat transfer between the fluid and wall surfaces was modeled using a constant heat flux boundary condition.

In addition, mesh independence tests and convergence criteria were verified to ensure the reliability of the numerical results. An optimal balance was established between mesh resolution, computational cost, and solution accuracy. A mesh independence study was conducted by comparing the average outlet air temperature and velocity for three mesh sizes: coarse (x nodes), medium (y nodes), and fine (z nodes). The relative difference between the medium and fine mesh results was found to be below 1.5%, indicating sufficient mesh convergence. The results obtained were used to comparatively evaluate the influence of channel height and mass flow rate on the thermal performance of the evaporator.

Results and Discussion

The temperature distributions within the evaporator at a channel height of 3 cm under different mass flow rates are shown in Figure 1. Under low-flow conditions (Figure 1.a), air could not effectively remove heat from the evaporator surface. Consequently, high localized surface temperatures (> 390 K) were observed, and the temperature was not uniformly distributed along the plate. This indicates an insufficient convective heat transfer. With an increased flow rate (Figure

1.b), the surface temperature distribution became more uniform; however, some hot spots remained, suggesting limited contact between the airflow and evaporator surface. When the air mass flow rate increased to 0.075 kgs^{-1} (Figure 1.c), heat was more efficiently removed from the evaporator surface owing to the sufficient flow rate. Thus, the temperature contours became more homogeneous. These results indicate that a channel height of 3 cm is adequate and provides effective cooling performance.

Figure 1.
Temperature contours for empty evaporator with channel height of 3 cm at different mass flow rates: a) 0.025 kgs^{-1}, b) 0.050 kgs^{-1}, and c) 0.075 kgs^{-1}.

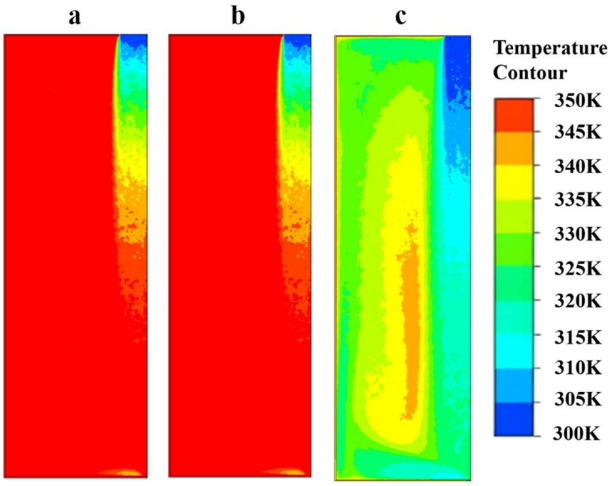

Figure 2 shows the temperature contours obtained when the evaporator height increased to 4 cm. In this case, the temperature profiles at all the flow rates were similar. Compared to the 3 cm channel height, the temperature was distributed over a wider surface area, although the average temperatures were slightly lower. A height of 4 cm allows more extensive contact between the fluid and the surface, resulting in more uniform heat transfer. However, the performance improvement over the 3 cm configuration was limited. Although a larger channel volume provides a more homogeneous air distribution, the contact ratio with the cooling surface decreases. Although the temperature values are lower than those in the 3 cm case, the efficiency difference remains marginal. A thermal equilibrium was achieved across the surface at a flow rate of 0.075 kgs^{-1}.

Figure 2.
Temperature contours for the empty evaporator with a channel height of 4 cm: a) 0.025 kgs^{-1}, b) 0.050 kgs^{-1}, and c) 0.075 kgs^{-1}.

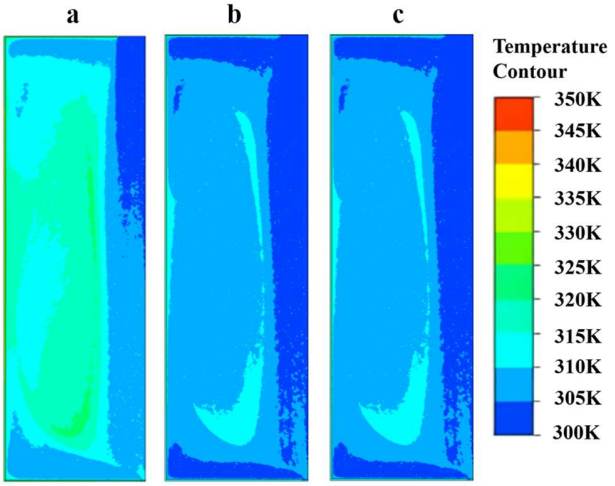

On the other hand, the temperature distributions obtained in the evaporator with a 5 cm channel height are similar to those observed at 4 cm (Figure 3). However, the increased height resulted in reduced flow velocity, which led to inadequate cooling in certain regions of the evaporator. Although the temperature was more widely distributed, it did not provide a performance advantage over the other two configurations. While a heat distribution similar to that of the 4 cm case was achieved, the overall cost increased.

The flow streamlines and direction of the air within the evaporator for a 3 cm channel height are shown in Figure 4. At 0.025 kgs-1, the streamlines are weak and tend to adhere closely to the surface. The flow exhibits limited motion near the wall, resulting in the formation of hotspots. At 0.050 kgs^{-1}, the energy flow increased, and the surface interaction improved, although the distribution remained nonuniform. At 0.075 kgs^{-1}, dense and uniform streamlines are observed throughout the evaporator. The flow reached a maximum velocity of 5 ms^{-1} and exhibited a strong interaction with the surface. In terms of the heat transfer performance, 0.075 kgs^{-1} was the most efficient operating condition (Figure 4c).

Figure 3.
Temperature contours for the empty evaporator with a channel height of 5 cm: a) 0.025 kgs^{-1}, b) 0.050 kgs^{-1}, and c) 0.075 kgs^{-1}.

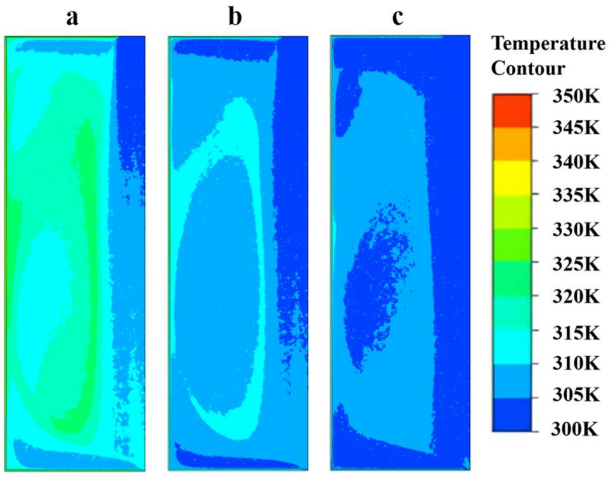

Figure 4.
Streamlines for the empty evaporator with a channel height of 3 cm: a) 0.025 kgs^{-1}, b) 0.050 kgs^{-1}, and c) 0.075 kgs^{-1}.

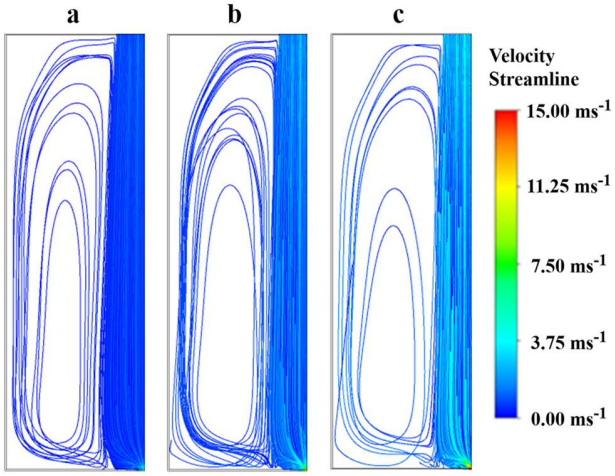

The streamlines for the 4 cm channel height configuration are presented in Figure 5. In this case, at all flow rates, the streamlines traveled farther from the surface, which weakened the convective heat transfer. Although increasing the flow rate slightly improves this behavior, the limited surface contact results in lower performance compared to the 3 cm configuration. The streamlines appeared freer and more detached from the surface, reducing the effective contact area. A larger channel volume decreased the flow density per unit mass flow, thereby preventing effective cooling.

Figure 5.
Streamlines for the empty evaporator with a channel height of 4 cm: a) 0.025 kgs^{-1}, b) 0.050 kgs^{-1}, and c) 0.075 kgs^{-1}.

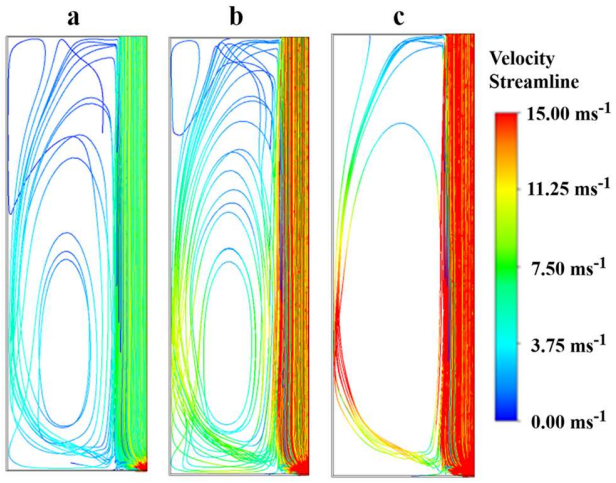

The streamline results for the 5 cm channel height are shown in Figure 6. At this height, particularly at lower flow rates, the flow slows down, and the amount of fluid reaching the surface decreases, resulting in a significantly reduced cooling performance. Although the increased channel height increases the production costs, it does not provide a meaningful improvement in the thermal performance.

Figure 6.
Streamlines for the empty evaporator with a channel height of 5 cm: a) 0.025 kgs^{-1}, b) 0.050 kgs^{-1}, and c) 0.075 kgs^{-1}.

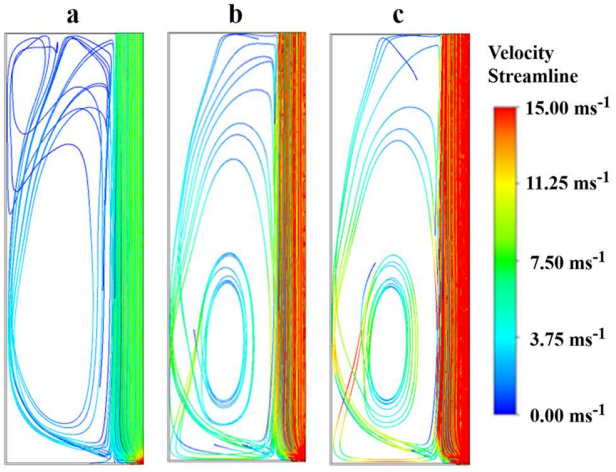

Figure 7 presents the average outlet velocities of the evaporator for three different channel heights. The graph shows that, as the mass flow rate increased, the outlet velocity also increased. However, at a channel height of 3 cm, the increase in the velocity was significantly steeper. In contrast, the 4 cm and 5 cm channels exhibit more gradual increases. This indicates that narrower channels provide a velocity advantage. The optimum

average velocity was obtained for the 3–0.075 kgs^{-1} configuration.

As shown in Figure 8, at a channel height of 3 cm, the airflow passed closer to the surface, resulting in a more effective heat transfer and consequently higher outlet air temperatures. In contrast, for channel heights of 4 and 5 cm, the outlet temperatures remained nearly the same and were found to be insufficient for drying purposes. This indicates that achieving optimal performance requires a combination of a high mass flow rate and low channel height. In terms of average outlet temperature, the 3 cm channel height demonstrated a significant advantage over the 4 cm and 5 cm configurations. These findings reveal that the airflow passing near the surface absorbs more heat and transports the thermal energy required for drying more efficiently.

Figure 7.
Average outlet velocity of the empty evaporator for three different channel heights.

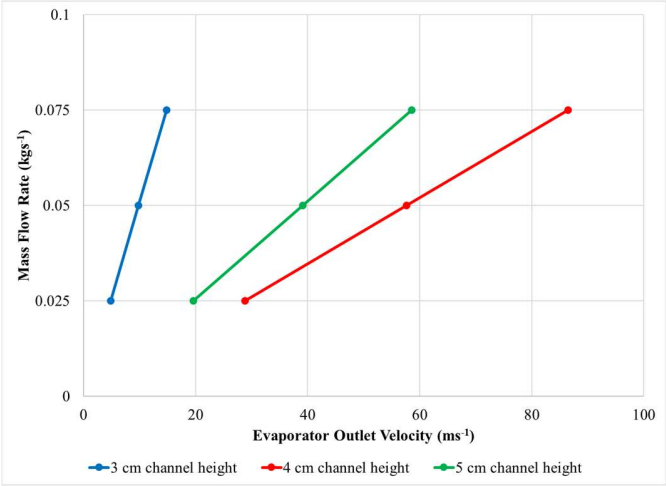

Figure 8.
Average outlet air temperature of the empty evaporator for three different channel heights.

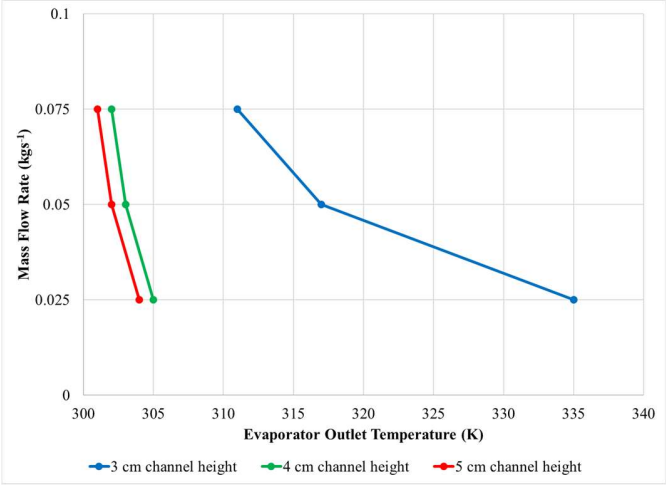

Conclusion

In this study, the effects of the channel height and air mass flow rate on the thermal and flow characteristics of the evaporator unit used in a photovoltaic-assisted solar drying system were comprehensively investigated using ANSYS Fluent, a numerical analysis method. Based on evaluations of the obtained temperature contours, streamlines, and performance graphs, the following key findings were derived:

- ✓ The channel height and airflow rate had a significant impact on the thermal performance of the system. In particular, at a channel height of 3 cm and flow rate of 0.075 kgs^{-1}, intense contact with the surface was achieved, resulting in efficient heat transfer from the evaporator.
- ✓ The temperature contours obtained at 3 cm exhibited a more homogeneous distribution and lower maximum temperatures than those of the other configurations. In particular, under high-flow conditions, no hotspots were observed, and the heat was distributed uniformly across the surface.
- ✓ According to the streamline analysis, increasing the flow rate at a channel height of 3 cm enhanced the contact between the fluid and surface, thereby maximizing convective heat transfer. In contrast, for heights of 4 cm and 5 cm, the airflow remained farther from the surface, limiting the heat transfer effectiveness.
- ✓ The highest performance in terms of the average outlet temperature and velocity was achieved with the 3–0.075 kgs^{-1} configuration. No significant improvements were observed at heights of 4 cm and 5 cm, whereas production costs increased without a corresponding gain in system efficiency.
- ✓ From an energy efficiency and economic sustainability perspective, the 3 cm channel height stands out as the optimal configuration. The 4 cm and 5 cm channel heights increased the production costs but did not meaningfully contribute to the thermal performance.

Accordingly, it is recommended to design the evaporator unit of the solar drying system with a 3 cm channel height operating at a flow rate of 0.075 kgs^{-1}. This configuration enhances both the system efficiency and resource utilization. These findings are expected to serve as valuable technical references for researchers and engineers for the development of similar solar-assisted drying systems.

Future Work

The numerical findings obtained in this study clearly demonstrate the effects of evaporator channel height and airflow rate on the performance of solar-assisted drying

systems. However, the scope was limited to the evaporator unit, which represents only a part of the overall system. In future work, a laboratory-scale experimental drying setup should be developed to validate the numerical results and compare the applied boundary conditions with the actual operating conditions. An experimental evaluation of the temperature and velocity distributions enhances the reliability of the simulations.

Furthermore, in future work, both energy and exergy analyses should be performed to comprehensively assess the thermodynamic performance of the drying system. To improve the reliability of the simulation results, an experimental prototype will be developed and validated under controlled laboratory conditions. Temperature and velocity measurements at the evaporator outlet will be compared with the CFD predictions. These analyses can help identify the thermal losses within the system and reveal areas with potential for improvement. Future studies should also focus on investigating the drying behavior of Rumex crispus (dockweed) or similar leafy products by examining the relationship between product characteristics, moisture content, and air temperature. Based on these findings, product-specific drying strategies can be developed to improve efficiency and product quality.

Peer-review: *Externally peer-reviewed.*

Author Contributions:

RY: Data collection/processing, data analysis and interpretation, visualization

RAO: Data analysis and interpretation, literature research, writing

JE: Consultant, main idea/planning, review, data interpretation

Conflict of Interest: *The authors have no conflicts of interest to declare.*

Financial Disclosure: *This study was supported by the Scientific Research Projects Coordination Unit of Kafkas University (Project Number 2023-FM-21).*

References

Abdullah A. S., Abou Al-sood M. M., Omara Z. M., Bek M. A. & Kabeel A. E. (2018) Performance evaluation of a new counter flow double pass solar air heater with turbulators. *Solar Energy*, *173*, 398–406. https://doi.org/10.1016/J.SOLENER.2018.07.073

Arpaci E., Atayılmaz Ö. & Gemici Z. (2024). Exploring Mathematical Modeling and CFD in Convective Drying of Fruits and Vegetables: A Review. *Food and Bioprocess Technology* *18*(4), 3195–3222. https://doi.org/10.1007/S11947-024-03627-2

Bal L. M., Satya S., Naik S. N. & Meda V. (2011). Review of solar dryers with latent heat storage systems for agricultural products. *Renewable and Sustainable Energy Reviews*, *15*(1), 876–880. https://doi.org/10.1016/J.RSER.2010.09.006

Barnwal P. & Tiwari G. N. (2008). Grape drying by using hybrid photovoltaic-thermal (PV/T) greenhouse dryer: An experimental study. *Solar Energy*, *82*(12), 1131–1144. https://doi.org/10.1016/J.SOLENER.2008.05.012

Belessiotis V. & Delyannis E. (2011). Solar drying. *Solar Energy*, *85*(8), 1665–1691. https://doi.org/10.1016/J.SOLENER.2009.10.001

El-Sebaii A. A. & Shalaby S. M. (2012). Solar drying of agricultural products: A review. *Renewable and Sustainable Energy Reviews*, *16*(1), 37–43. https://doi.org/10.1016/J.RSER.2011.07.134

Ertekin C. & Yaldiz O. (2004). Drying of eggplant and selection of a suitable thin layer drying model. *Journal of Food Engineering*, *63*(3), 349–359. https://doi.org/10.1016/J.JFOODENG.2003.08.007

Esper A. & Mühlbauer W. (1998). Solar drying - an effective means of food preservation. *Renewable Energy*, *15*(1–4), 95–100. https://doi.org/10.1016/S0960-1481(98)00143-8

Fadhel M. I., Sopian K. & Daud W. R. W. (2010). Performance analysis of solar-assisted chemical heat-pump dryer. *Solar Energy*, *84*(11), 1920–1928. https://doi.org/10.1016/J.SOLENER.2010.07.001

Fudholi A., Sopian K., Ruslan M. H., Alghoul M. A. & Sulaiman M. Y. (2010). Review of solar dryers for agricultural and marine products. *Renewable and Sustainable Energy Reviews*, *14*(1), 1–30. https://doi.org/10.1016/J.RSER.2009.07.032

Fudholi Ahmad, Sopian K., Othman M. Y. & Ruslan M. H. (2014). Energy and exergy analyses of solar drying system of red seaweed. *Energy and Buildings*, *68*(PARTA), 121–129. https://doi.org/10.1016/J.ENBUILD.2013.07.072

Ghafar H., Yusoff H., Nasir S. M. F. S. A., Ghani K. D. A. & Ismail M. A. (2025). PERFORMANCE EVALUATION OF NATURAL AND FORCED CONVECTION IN SOLAR DRYERS FOR MULLET FISH. *Jurnal Teknologi (Sciences & Engineering)*, *87*(1), 43–52. https://doi.org/10.11113/JURNALTEKNOLOGI.V87.22448

Güler H. Ö., Sözen A., Tuncer A. D., Afshari F., Khanlari A., Şirin C. & Gungor A. (2020). Experimental and CFD survey of indirect solar dryer modified with low-cost iron mesh. *Solar Energy*, *197*, 371–384. https://doi.org/10.1016/J.SOLENER.2020.01.021

Hassan A., Joardder M. U. H. & Karim A. (2025). A CFD integrated drying model for improving drying conditions in industry Scale dryers. *Thermal Science and Engineering Progress*, *61*, 103533. https://doi.org/10.1016/J.TSEP.2025.103533

Kerse A. Y., Embiale D. T. & Gunjo D. G. (2025). Dehydration of red chilli using an indirect type forced convection solar dryer integrated with thermal energy storage. *International Journal of Thermofluids*, *26*, 101045. https://doi.org/10.1016/J.IJFT.2024.101045

Keshani S., Montazeri M. H., Daud W. R. W. & Nourouzi M. M. (2015). CFD Modeling of Air Flow on Wall Deposition in Different Spray Dryer Geometries. *Drying Technology*, *33*(7), 784–795. https://doi.org/10.1080/07373937.2014.966201;WGROUP:STRING:PUBLICATION

Mustayen A. G. M. B., Mekhilef S. & Saidur R. (2014). Performance study of different solar dryers: A review. *Renewable and Sustainable Energy Reviews*, *34*, 463–470. https://doi.org/10.1016/J.RSER.2014.03.020

Ozer R. A. (2025). Heat sink optimization with response surface methodology for single phase immersion cooling. *International Journal of Heat and Fluid Flow*, *112*, 109745. https://doi.org/10.1016/J.IJHEATFLUIDFLOW.2025.109745

Sanghi A., Ambrose R. P. K. & Maier D. (2018). CFD simulation of corn drying in a natural convection solar dryer. *Drying Technology*, *36*(7), 859–870. https://doi.org/10.1080/07373937.2017.1359622;WGROUP:STRING:PUBLICATION

Shalaby S. M., Bek M. A. & El-Sebaii A. A. (2014a). Solar dryers with PCM as energy storage medium: A review. *Renewable and Sustainable Energy Reviews*, *33*, 110–116. https://doi.org/10.1016/J.RSER.2014.01.073

Shalaby S. M., Bek M. A. & El-Sebaii A. A. (2014b). Solar dryers with PCM as energy storage medium: A review. *Renewable and Sustainable Energy Reviews*, *33*, 110–116. https://doi.org/10.1016/J.RSER.2014.01.073

Sharma A., Chen C. R. & Vu Lan N. (2009). Solar-energy drying systems: A review. *Renewable and Sustainable Energy Reviews*, *13*(6–7), 1185–1210. https://doi.org/10.1016/J.RSER.2008.08.015

Sodha M. S. & Chandra R. (1994). Solar drying systems and their testing procedures: A review. *Energy Conversion and Management*, *35*(3), 219–267. https://doi.org/10.1016/0196-8904(94)90004-3

Souza A. S., Souza Pinto T. C., Sarkis, A. M., Pádua T. F. de & Béttega, R. (2023). Convective drying of iron ore fines: A CFD model validated for different air temperatures and air velocities. *Drying Technology*, *41*(15), 2431–2446. https://doi.org/10.1080/07373937.2023.2252050;JOURNAL:JOURNAL:LDRT20;WGROUP:STRING:PUBLICATION

Tu Q., Ma, Z. & Wang H. (2023). Investigation of wet particle drying process in a fluidized bed dryer by CFD simulation and experimental measurement. *Chemical Engineering Journal*, *452*, 139200. https://doi.org/10.1016/J.CEJ.2022.139200

Yakut R., Yakut K., Yeşildal F. & Karabey A. (2016). Experimental and Numerical Investigations of Impingement Air Jet for a Heat Sink. *Procedia Engineering*, *157*, 3–12. https://doi.org/10.1016/J.PROENG.2016.08.331